

広島大学学術情報リポジトリ

Hiroshima University Institutional Repository

Title	Biomolecule detection based on Si single-electron transistors for highly sensitive integrated sensors on a single chip
Author(s)	Kudo, Takashi; Nakajima, Anri
Citation	Applied Physics Letters , 100 (2) : 023704
Issue Date	2012
DOI	10.1063/1.3676664
Self DOI	
URL	http://ir.lib.hiroshima-u.ac.jp/00034091
Right	(c) 2012 American Institute of Physics
Relation	



Biomolecule detection based on Si single-electron transistors for highly sensitive integrated sensors on a single chip

Takashi Kudo and Anri Nakajima^{a)}

Research Institute for Nanodevice and Bio Systems, Hiroshima University, 1-4-2 Kagamiyama, Higashihiroshima 739-8527, Japan

(Received 12 October 2011; accepted 22 December 2011; published online 12 January 2012)

Biomolecule detection was achieved using a Si single-electron transistor (SET) for highly-sensitive detection. A multiple-island channel-structure was used for the SET to enable room-temperature operation and to increase sensitivity. Coulomb oscillation shifted against the gate voltage due to biotin-streptavidin binding. Coulomb oscillation has a possibility to increase transconductance (g_m), and a higher g_m leads to greater sensitivity to a charged target. Since a Si structure is important for integrating label-free-biomolecule and/or ion sensors into large-scale-integrated circuits, a Si SET with multiple islands should enable the integration of a sensor system on a single chip for multiplexed detections and simultaneous diagnoses. © 2012 American Institute of Physics. [doi:10.1063/1.3676664]

The detection and quantification of chemical and biological species are central to many areas of healthcare and life sciences. Field effect transistors (FETs) are sophisticated devices used for the label-free detection of charged molecules.¹ Ion-sensitive field effect transistors (ISFETs) are a typical example. Furthermore, biosensors based on FETs have recently been developed for the detection of DNA, proteins, and viruses.^{2–7} FETs measure changes in charge accompanied by specific molecular recognition events on the gate insulator surface. Highly sensitive detection of target ions or biomolecules has been obtained using a nanowire channel in FET sensors.^{8–11} However, FET sensors with even higher detection sensitivity are preferable, especially for dilute solutions of targets, which have relatively high electrical noise levels.

Single electron transistors (SETs) are a promising candidate for highly sensitive detection because using Coulomb oscillations has a possibility to result in high resolving power for ion and/or biomolecule concentrations. Owing to the difficulties in room temperature (RT) operation of SETs, there have been no reports of an SET-based biosensor.

We previously developed a pH sensor based on a Si SET with a multiple-island channel structure for ion detection.¹² It operates effectively at RT. We have now developed a biomolecule sensor based on a Si SET that also has a multiple-island channel structure. We clarified the advantages of a multiple-island structure and proved the feasibility of highly sensitive biomolecule and ion sensors. The Si structure enables the use of existing large-scale integration (LSI) technology for chip fabrication. The fabricated FET sensors can be integrated on a single chip for simultaneous detection and quantification of various ions and/or biomolecules.

We fabricated SETs with multiple Coulomb islands serially connected in a silicon-on-insulator (SOI) layer. They have 11 islands and a channel length of $3\ \mu\text{m}$. The fabrica-

tion process and device structure are similar to those of our previously reported ISFET using a Si SET (Ref. 12) with a slight modification. A p-type (B-doped) SOI (100) wafer ($8.5\text{--}11.5\ \Omega\ \text{cm}$) was used. The thicknesses of the top silicon layer and buried oxide on the SOI wafers were 50 and 400 nm, respectively. Doping of the top silicon layer was carried out by POCl_3 diffusion at $850\ ^\circ\text{C}$ for 30 min. The doping level was about $3.5 \times 10^{20}\ \text{cm}^{-3}$. The fabrication process of a channel region includes electron beam lithography and dry etching using an electron-cyclotron resonance etcher with the resist pattern as a mask. Subsequent isotropic wet etching in a solution of $\text{NH}_4\text{OH}/\text{H}_2\text{O}_2/\text{H}_2\text{O}$ at $80\ ^\circ\text{C}$ reduced the dimensions of the device, and the damage introduced during the dry etching process.¹³ The nanowire region (constricted region in the channel) acts as a tunnel barrier due to the quantum-size effect.¹⁴ A scanning electron micrograph of the channel region of a fabricated Si SET with 11 islands after dry etching is shown in Fig. 1(a).

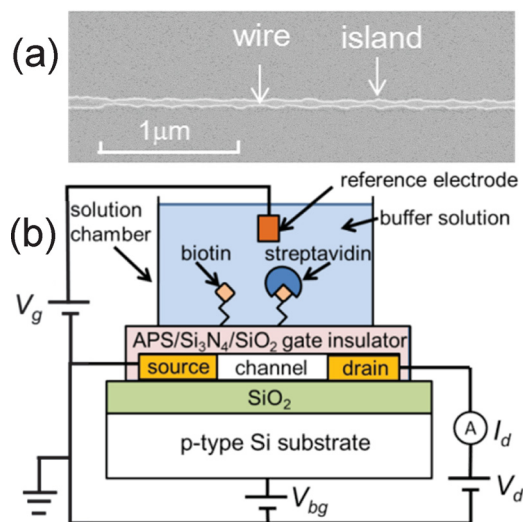


FIG. 1. (Color online) (a) Scanning electron micrograph of fabricated Si single-electron transistor (SET) with 11 islands after dry etching. (b) Schematic diagram of measurement system.

^{a)} Author to whom correspondence should be addressed. Electronic mail: anakajima@hiroshima-u.ac.jp.

Next, we fabricated $\text{Si}_3\text{N}_4/\text{SiO}_2$ stacked gate insulators. A layer of SiO_2 , about 10 nm thick, was thermally grown at 850°C in a dry atmosphere followed by the deposition of about 90-nm-thick Si_3N_4 by low-pressure chemical vapor deposition at 750°C . The final thickness of the top Si layer was estimated to be about 35 nm (excluding the thickness of the SiO_2). The final width of the nanowire barrier region was about 10 nm and the length was 150–200 nm. The wider region of the island width was about 30 nm and the island length was 50–100 nm. After contact holes and Al electrodes were fabricated, the samples were annealed at 400°C in an H_2 atmosphere.

A schematic diagram of our measurement system is shown in Fig. 1(b). A solution chamber was attached to the $\text{Si}_3\text{N}_4/\text{SiO}_2$ gate insulator. The channel region including all barriers and islands in the SET was inside the solution chamber region. The diameter of the chamber was 0.5 cm. An Au reference electrode was used to control the gate voltage (V_g) of the SET through a buffer solution.

The $\text{Si}_3\text{N}_4/\text{SiO}_2$ gate insulator surface was chemically modified. To remove organic contamination, the surface of the Si_3N_4 layer was cleaned in a solution of $\text{H}_2\text{O}/\text{H}_2\text{O}_2/\text{NH}_4\text{OH}$ (weight ratio of 18:1:1) at 80°C for 10 min.¹⁵ After being rinsed with pure water, the surface was cleaned again with 1 M NaOH for 1 h at RT.⁷ To silanize the Si_3N_4 surface [i.e., to form an aminopropylsiloxane (APS) surface], the surface was soaked in 2 wt.% 3-aminopropyltriethoxysilane (APTES) in anhydrous toluene⁷ at 60°C for 10 min. It was then rinsed in anhydrous toluene and dried immediately in vacuum at 110°C for 1 h.⁷ After silanization, biotin (250 $\mu\text{g}/\text{ml}$) was reacted with the APS-terminated Si_3N_4 surface at RT for 30 min to obtain a biotinylated surface. Finally, the biotinylated surface was reacted with 10- $\mu\text{g}/\text{ml}$ streptavidin for 30 min. The electrical characteristics were measured using a semiconductor parameter analyzer (B1500A, Agilent).

Figure 2 shows the results of biomolecule detection using the well-known ligand-receptor binding of biotin-streptavidin. To avoid the problem of Debye screening, we chose the ion concentrations in the buffer solution such that the Debye screening length was sufficiently long to enable detection and sufficiently short to screen unbound biomolecules.¹⁶ At the same time, the pH of the buffer solutions was set to 8.0–8.2 since the isoelectric point of streptavidin is pH 5–6.¹⁰ Therefore, the streptavidin was negatively charged in the buffer solution. The drain current (I_d)-gate voltage (V_g) characteristics were measured before and after the biotinylation of the APS-terminated surface and after the subsequent addition of 10- $\mu\text{g}/\text{ml}$ streptavidin to the biotinylated surface. For each surface modification, the electrical characteristics were obtained five times to confirm reproducibility. As can be seen in Fig. 2(a), the I_d - V_g curve differed for each surface modification. For the reason described later, we evaluated the V_g shift in each curve on the left side of the peak. At the half-maximum peak current, the V_g value ($V_{g, \text{half}}$) shifted -220 mV due to the attachment of biotin to the APS-terminated surface, which is consistent with the positive charge of biotin [Fig. 2(b)]. In contrast, the successive addition of 10- $\mu\text{g}/\text{ml}$ streptavidin resulted in an increase in $V_{g, \text{half}}$ (the V_g shift = $+150\text{ mV}$), which is consistent with the negative charge of streptavidin. If we fixed the V_g ($=5.95\text{ V}$)

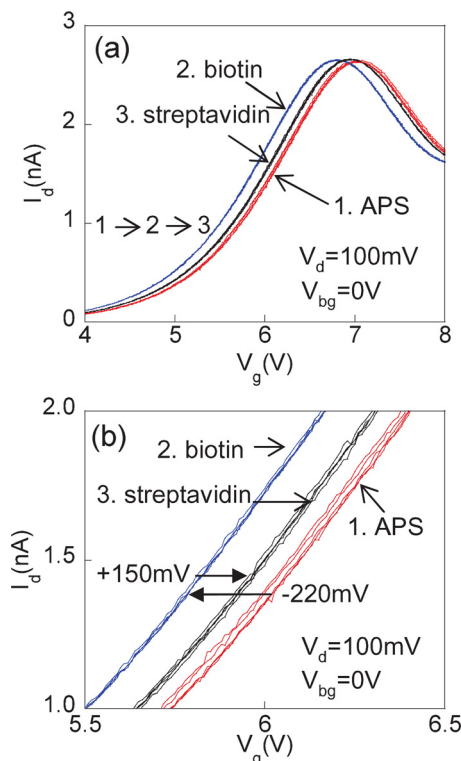


FIG. 2. (Color online) Drain current (I_d) vs. gate voltage (V_g) characteristics of SET with multiple islands for biotin-streptavidin binding at room temperature. Drain-source voltage (V_d) was fixed at 100 mV. Back-gate voltage (V_{bg}) was fixed at 0 V. The results were for 10- $\mu\text{g}/\text{ml}$ streptavidin. (b) Curves in V_g region from 5.5 to 6.5 V for (a).

at $V_{g, \text{half}}$ for APS-terminated surface, we can observe correspondingly that I_d increases (the average I_d shift = $+350\text{ pA}$) after the attachment of biotin and then decreases (the average I_d shift = -220 pA) after the successive binding of streptavidin. These experimental results demonstrate the achievement of biomolecule detection based on a Si SET using the binding of biotin-streptavidin.

The advantage of the use of an SET for biomolecular and/or ion sensing is as follows. If the barrier conductance (drain conductance) depends on V_g , the Coulomb oscillations are modulated and weighted by the variation in the barrier conductance. If the barrier conductance increases with V_g , the transconductance (g_m) in the SET possibly becomes larger than that of the barrier itself [Fig. 3(a)]. In this case, g_m can be larger, especially around a left-side V_g value near the half-maximum peak current. A larger g_m leads to higher sensitivity to a charged target. If SETs with a sufficiently doped channel were used in accumulation mode, there is an advantage that targets can be detected only from the change in I_d at $V_g = 0\text{ V}$ (it is not necessary to increase V_g). When MOSFETs with a sufficiently doped channel were used in accumulation mode, a metal-like conduction appeared, in which the drain conductance was almost constant against V_g . However, such a MOSFET cannot be used for biomolecule detection because $g_m = 0$ [Fig. 3(b)]. Even in this case, if the channel structure was changed to that of an SET, Coulomb oscillation appeared, and g_m increased [Fig. 3(b)]. In the inversion mode, the advantage of detecting targets at $V_g = 0\text{ V}$ cannot be obtained usually due to the high threshold voltage (V_{th}).

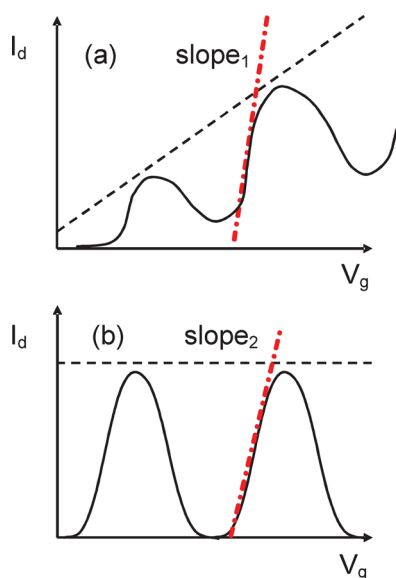


FIG. 3. (Color online) Schematic view illustrating reason for highly sensitive detection of charged target when SET was used for case in which barrier conductance (drain conductance) increases with gate voltage (V_g) (a) and for case in which barrier conductance was constant (b). Broken lines show drain current vs. gate voltage characteristics of nanowire barrier region. Dash-dotted lines show steepest slope of drain current (I_d) against V_g .

Using a multiple-island channel structure in SETs has two advantages for biomolecular and/or ion sensing. One is high-temperature operation. For ion and/or biomolecule sensing, RT operation is strongly required. To achieve RT operation of an SET with a single island, the island size should be less than 10 nm, which is difficult even with present LSI technologies.¹⁷ A serially connected multiple-island channel structure overcomes this difficulty because the effective total capacitance of an island decreases, which leads to an increase in the charging energy.^{14,17,18} The other advantage is that the multiple-island system increases the sensitivity: I_d in the SET easily changes with the dilute target concentration because it changes even if only one target molecule attaches to one of the islands (Fig. 4). Receptor molecules on the island surfaces are attached by surface modifications. If a target molecule happens to meet with one of the receptor molecules, specific binding occurs, and the effective gate voltage in the SET changes, leading to a change in the drain current. The probability of a target molecule meeting a receptor molecule is larger in a multiple-island channel structure than in a single-island channel structure.

In summary, biomolecule detection was achieved using a Si single-electron transistor for highly sensitive detection. After chemical modification of the $\text{Si}_3\text{N}_4/\text{SiO}_2$ gate insulator surface with 3-aminopropyltriethoxysilane and biotin, streptavidin was detected on the basis of a clear shift in the gate voltage at the half-maximum peak current of the Coulomb

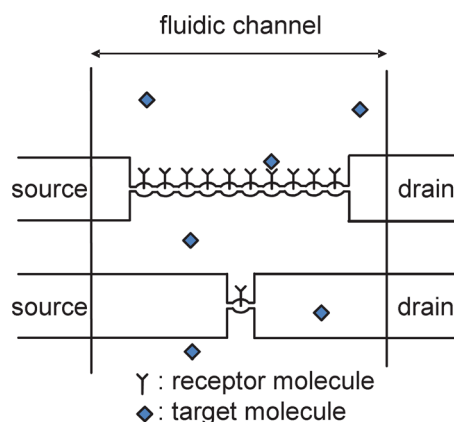


FIG. 4. (Color online) Schematic view illustrating reason for highly sensitive detection of charged target by using multiple-island channel structure.

oscillation. Coulomb oscillation has a possibility to increase the transconductance (g_m), and a larger g_m leads to higher sensitivity to a charged target. A channel structure with serially connected islands can operate at room temperature and has higher sensitivity. Since a Si structure enables label-free-biomolecule and/or ion sensors to be integrated into an LSI chip, a Si SET with multiple islands should enable the integration of a sensor system on a single chip for multiplexed detections and simultaneous diagnoses.

- ¹P. Bergveld, *IEEE Trans. Biomed. Eng.* **19**, 342 (1972).
- ²F. Patolsky, G. Zheng, O. Hayden, M. Lakadamyali, X. Zhuang, and C. M. Lieber, *Proc. Natl. Acad. Sci. U.S.A.* **101**, 14017 (2004).
- ³W. U. Wang, C. Chen, K. Lin, Y. Fang, and C. M. Lieber, *Proc. Natl. Acad. Sci. U.S.A.* **102**, 3208 (2005).
- ⁴K. Park, M. Kim, and S. Choi, *Biosens. Bioelectron.* **20**, 2111 (2005).
- ⁵E. Stern, J. F. Klemic, D. A. Routenberg, P. N. Wyrembak, D. B. Turner-Evans, A. D. Hamilton, D. A. LaVan, T. M. Fahmy, and M. A. Reed, *Nature* **445**, 519 (2007).
- ⁶M. Gotoh, E. Tamiya, I. Karube, and Y. Kagawa, *Anal. Chim. Acta* **187**, 287 (1986).
- ⁷T. Sakata, M. Kamahori, and Y. Miyahara, *Jpn. J. Appl. Phys.* **44**, 2854 (2005).
- ⁸T. Kudo, T. Kasama, T. Ikeda, Y. Hata, S. Tokonami, S. Yokoyama, T. Kikkawa, H. Sunami, T. Ishikawa, M. Suzuki, K. Okuyama, T. Tabei, K. Ohkura, Y. Kayaba, Y. Tanushi, Y. Amemiya, Y. Cho, T. Monzen, Y. Murakami, A. Kuroda, and A. Nakajima, *Jpn. J. Appl. Phys.* **48**, 06FJ04 (2009).
- ⁹G. Zheng, F. Patolsky, Y. Cui, W. U. Wang, and C. M. Lieber, *Nat. Biotechnol.* **23**, 1294 (2005).
- ¹⁰Y. Cui, Q. Wei, H. Park, and C. M. Lieber, *Science* **293**, 1289 (2001).
- ¹¹O. Knopfmacher, A. Tarasov, W. Fu, M. Wipf, B. Niesen, M. Calame, and C. Schönenberger, *Nano Lett.* **10**, 2268 (2010).
- ¹²T. Kudo and A. Nakajima, *Appl. Phys. Lett.* **98**, 123705 (2011).
- ¹³A. Nakajima, H. Aoyama, and K. Kawamura, *Jpn. J. Appl. Phys., Part 2* **33**, L1796 (1994).
- ¹⁴A. Nakajima, Y. Ito, and S. Yokoyama, *Appl. Phys. Lett.* **81**, 733 (2002).
- ¹⁵N. A. Lapin and Y. J. Chabal, *J. Phys. Chem. B* **113**, 8776 (2009).
- ¹⁶S. Hideshima, H. Einati, T. Nakamura, S. Kuroiwa, Y. S. Diamond, and T. Osaka, *J. Electron. Soc.* **157**, J410 (2010).
- ¹⁷K. Ohkura, T. Kitade and A. Nakajima, *J. Appl. Phys.* **98**, 124503 (2005).
- ¹⁸T. Kitade, K. Ohkura, and A. Nakajima, *Appl. Phys. Lett.* **86**, 123118 (2005).